AAS 11-210

CLUSTER FLIGHT FOR FRACTIONATED SPACECRAFT

Leonel Mazal* **and Pini Gurfil†**

Fractionated spacecraft constitutes a satellite design methodology wherein the functional capabilities of a single monolithic satellite are distributed among multiple free-flying, wirelessly-communicating modules. One of the main challenges of a fractionated spacecraft system is cluster flight, i.e. keeping the various modules within a bounded distance, typically less than 100 km, for the entire mission lifetime. This paper presents a methodological development of cluster flight algorithms for fractionated spacecraft systems. To obtain distance-bounded relative motion, a new constraint on the initial conditions of the modules is developed. A concomitant analytical bound on the relative distance between the modules is proven based on a design model assuming time-invariance of the environmental perturbations. It is then shown that if the actual astrodynamical model includes other, possibly time-varying effects, mild drifts between the modules are obtained. Furthermore, this paper presents a cluster establishment algorithm for tracking a given nominal orbit, whose characteristics satisfy the previously-develop no-drift constraint. This algorithm provides fuel balancing among the maneuvering modules as well as minimization of the total fuel consumption. Numerical simulations using realistic astrodynamical models are used to validate the analysis.

INTRODUCTION

Standard spacecraft designs are comprised of functional modules assembled in a single monolithic structure. When unexpected faults occur, it is difficult for the spacecraft to adequately respond in order to continue the pre-planned mission, and significant losses (both technical and financial) are unavoidable. For instance, if the payload fails, the whole system becomes unserviceable and substitution of the entire spacecraft is required in order to complete the mission. This operation is expensive and time demanding; it would be easier to replace only the payload module than launch a completely new satellite. This idea gives rise to the emerging concept termed *fractionated spacecraft*. Some of the main ideas on which fractionated spacecraft rely upon were formally introduced by Brown and Eremenko.[1] Later works described general architectures for these systems and discussed both advantages and disadvantages compared to conventional architectures.[2]

Fractionated spacecraft consist of multiple free-flying physically-separated, yet functionally linked modules interacting through wireless cross-links to form a single virtual

*Graduate Student, Faculty of Aerospace Engineering, Technion - Israel Institute of Technology, Haifa 32000, Israel. Email: leomazal@technion.ac.il

†Associate Professor, Faculty of Aerospace Engineering, Technion - Israel Institute of Technology, Haifa 32000, Israel. Associate Fellow AIAA. Email: pgurfil@technion.ac.il

platform. The modules are heterogeneous, having one or more pre-determined functions: Navigation, attitude control, power generation and payload operation, among others. Wireless communication would enable the modules to share data, transmit resources, and exert remote commands. Unlike traditional spacecraft formation flying applications, the modules do not necessarily have to operate in a tightly-controlled formation; instead, due to communication links, they are required to maintain bounded relative distances, typically smaller than about 100 kilometers, for the entire mission lifetime. This concept is termed *cluster flight*. To accomplish cluster flight it is necessary to develop implementable, extendable, and robust cluster establishment and cluster-keeping strategies.

Without control forces, two initially close satellites – a *chief* and a *deputy* – rapidly drift apart due to differential accelerations. It is thus imperative to identify orbits on which the satellites or satellite modules remain within some pre-specified relative distance for a relatively long interval of time. These orbits can considerably reduce the propellent mass required for orbit maintenance and render the entire mission much more cost-effective. In the unperturbed two-body problem, such orbits can be simply designed by imposing energy matching.[3] However, when perturbations are present, other conditions for mitigating the relative drift must be found.

The most significant perturbations affecting low Earth-orbit satellites are the Earth oblateness and drag. Many works have dealt with modeling relative motion under these perturbations. Ross assumed a fixed circular reference orbit to obtain linearized equations of J_2-perturbed relative motion. However, since J_2 induces nodal precession and apsidal rotation, the resulting model is only valid for a very short time.[4] Vadali developed analytical expressions for the relative motion between J_2-perturbed satellites utilizing the unit-sphere approach.[5] Sedwick and Schweighart derived a linearized model for relative motion under J_2 perturbations for satellites moving in almost-circular orbits.[6] By using a geometric method, Gim and Alfriend obtained a state transition matrix for the relative motion between satellites on elliptic orbits subject to J_2 effects.[7,8] Higher-order models for J_2-perturbed motion were suggested by Sengupta et al.[9] Based on the Gauss Variational Equations (GVE), Kechichian derived a nonlinear relative motion model subject to drag and J_2 effects.[10]

There are other works that develop relative initial states for mitigating drifts among satellites as well as strategies to maintain these states. For instance, Lovell and Tragesser developed an algorithm for multi-impulsive guidance maneuvers using a parameterized version of the Hill-Clohessy-Wiltshire equations.[11] Vaddi et al. proposed a two-impulse maneuver scheme for formation reconfiguration using a two-body setup.[12] Others determined constraints leading to J_2 secular effect mitigation for relative orbits, and derived an optimal multi-impulsive scheme to establish the formations.[13,14] Mishne suggested a satellite relative motion model using differential mean orbital elements for two satellites flying in proximity subject to J_2 and drag. Using the GVE, optimal and periodic velocity vector corrections to compensate for the relative drift were developed.[15] Beigelman and Gurfil derived an algorithm for spacecraft formationkeeping using impulsive maneuvers. The algorithm minimizes the squared l^2-norm of the total ΔV for balancing the fuel consumption

of the satellites.[16]

This work is aimed at determining natural distance-bounded relative orbits and concomitant cluster establishment and cluster-keeping methods for long-term cluster flight. To that end, new design guidelines for generating relative initial states guaranteeing distance-bounded relative motion are developed. Using an astrodynamical design model comprised of zonal harmonics and a time-independent drag force, an analytical upper bound for the maximal possible distance between satellites is provided. Adding other effects to the astrodynamical design model does not significantly violate the analytically-predicted maximal distances. To maintain cluster flight for the entire missions lifetime, the current paper presents cluster establishment and cluster-keeping algorithms minimizing fuel consumption. These algorithms determine bi-impulsive maneuvers that enable fractionated spacecraft modules to attain relative states satisfying distance-keeping constraints under realistic astrodynamical modeling including the complete gravitational potential, drag, solar radiation pressure, lunisolar attraction, tides and relativistic effects.

DISTANCE-BOUNDED NATURAL ORBITS

The motion of Earth-orbiting artificial satellites is mainly governed by gravitational forces; in case of low Earth orbit satellites, drag may be significant as well. Earth's gravitational field is quite different from that predicted by the two-body problem – it is highly perturbed due to the non-uniform mass distribution of the planet. Other perturbations of importance are solar radiation pressure and lunisolar attraction. Minor effects include tides and relativity.

The following analysis develops a method for mitigating the relative distance drift between two fractionated spacecraft modules, $\mathcal{C}$ and $\mathcal{D}$, considering zonal harmonics and drag as a design model, to be later extended and validated using numerical tools. First, an Earth-Centered Inertial (ECI) coordinate system is defined in the following standard manner: The fundamental plane is the equatorial plane; the $\hat{\mathbf{x}}$-axis points towards the vernal equinox, the $\hat{\mathbf{z}}$-axis points towards the geographic north pole, and the $\hat{\mathbf{y}}$-axis completes the dextral triad. The vector $\mathbf{r} = [x, y, z]^T$ denotes the position in the ECI frame and $\mathbf{v} = d\mathbf{r}/dt$ is the velocity. Furthermore, the set of classical orbital elements is defined as $\boldsymbol{\alpha} \triangleq [a,\ e,\ i,\ \omega,\ f,\ \Omega]^T$, where a is the semimajor axis, e is the eccentricity, i is the inclination, ω is the argument of perigee, f is the true anomaly, and Ω is the right ascension of the ascending node (RAAN).

The gravitational potential field is modeled by an infinite series including zonal, sectorial, and tesseral harmonics. The zonal harmonics account for axially-symmetric deviations from an ideal sphere, where the polar axis is considered as the axis of rotation. The zonals represent the most significant gravitational perturbations for artificial satellites, due to their secular and long-periodic effects on the orbital elements. The potential per unit-mass of the zonal harmonics including the main Newtonian gravitational term, written in ECI coordinates, is given by:

$$\Phi(\mathbf{r}) = -\frac{\mu}{r}\left[1 - \sum_{n=2}^{\infty} J_n \left(\frac{R_{eq}}{r}\right)^n P_n\left(\frac{z}{r}\right)\right] \tag{1}$$

where $r \triangleq \|\mathbf{r}\|$, P_n are Legendre polynomials of order n, J_n are the zonal harmonics coefficients, R_{eq} denotes the equatorial radius of the Earth, and μ is the gravitational parameter. From Eq. (1), it is seen that the potential Φ does not depend explicitly on time t, and consequently neither its gradient, $\nabla\Phi$.

The specific force generated by the atmospheric drag can be modeled as

$$\mathbf{d}_{Dr} = -\frac{1}{2\,m}\,\rho\,S\,C_D\;(\mathbf{v}-\mathbf{v}_{atm})\;\|\mathbf{v}-\mathbf{v}_{atm}\| \tag{2}$$

where ρ is atmospheric density at $\mathbf{r}$, S is the cross-sectional area, C_D is the drag coefficient defined with respect to the cross-sectional area, and m is the mass. The vector $\mathbf{v}_{atm}$ is the velocity of the atmosphere at $\mathbf{r}$; when resolved in ECI coordinates, this velocity satisfies $\mathbf{v}_{atm} = [0,\ 0,\ \Psi_E]^T \times \mathbf{r}$, where Ψ_E is the Earth spin rate about its polar axis, i.e.

$$\Psi_E = \frac{2\pi}{1 \text{ sidereal day}}$$

Including drag and zonal harmonics, the equations of motion of a spacecraft, written in ECI coordinates, are given by:

$$\ddot{\mathbf{r}} = -\nabla\Phi\Big|_{ECI} + \mathbf{d}_{Dr}\Big|_{ECI} \tag{3}$$

In the following development, the subscripts $(\cdot)_{\mathcal{C}}$ and $(\cdot)_{\mathcal{D}}$ will denote quantities related to the chief and deputy, respectively. If the initial state of $\mathcal{C}$ is given, the following proposition provides a method to obtain initial conditions for $\mathcal{D}$ such that the resulting relative motion will be distance-bounded. This proposition is based on the following observations: Since the initial orbital elements of the chief, $\boldsymbol{\alpha}_{\mathcal{C}}(t_0)$, are known, one can determine the maximal speed of $\mathcal{C}$, i.e. $V_{\max} = \max_t \|\mathbf{v}_{\mathcal{C}}(t)\|$, and the maximal equatorial projection of the position vector of $\mathcal{C}$, given by $\eta_{\max} = \max_t \eta(t)$, where $\eta(t) = \sqrt{x(t)^2 + y(t)^2}$.

Proposition 1 *Consider two satellites, $\mathcal{C}$ and $\mathcal{D}$, having identical constant ballistic coefficients, i.e.*

$$\frac{C_{D_{\mathcal{C}}} S_{\mathcal{C}}}{m_{\mathcal{C}}} = \frac{C_{D_{\mathcal{D}}} S_{\mathcal{D}}}{m_{\mathcal{D}}} = \textit{const.} \tag{4}$$

Assume that ρ is time-independent and axially-symmetric with respect to the Earth's polar axis, i.e. $\rho = \rho(r,z)$, and that $\boldsymbol{\alpha}_{\mathcal{C}}(t_0)$ is given. If the satellites $\mathcal{C}$ and $\mathcal{D}$ are subject to the equations of motion (3)*, with the gravitational potential as in Eq.* (1)*, and have initial conditions that satisfy the constraint:*

$$\boldsymbol{\alpha}_{\mathcal{D}}(t_0) = \boldsymbol{\alpha}_{\mathcal{C}}(t_0) + \int_{t_0}^{t_0+\Delta t} \dot{\boldsymbol{\alpha}}_{\mathcal{C}}\,\mathrm{d}t + \begin{bmatrix} \mathbf{0}_{5\times 1} \\ \Delta\Omega \end{bmatrix} \tag{5}$$

then the distance between $\mathcal{C}$ and $\mathcal{D}$ satisfies

$$\|\mathbf{r}_{\mathcal{D}}(t) - \mathbf{r}_{\mathcal{C}}(t)\| < V_{\max}\,|\Delta t| + 2\,\eta_{\max}\sin\left(\frac{|\Delta\Omega|}{2}\right) \tag{6}$$

where Δt is any given interval of time, $\mathbf{0}_{5\times1}$ denotes a five-dimensional zeros vector, and $\Delta\Omega = \Omega_{\mathcal{D}}(t_0) - \Omega_{\mathcal{C}}(t_0 + \Delta t) = \text{const.},\ \forall\Delta t,\ \forall t_0$ is any given differential RAAN.

Proof To prove Proposition 1, consider a fictitious satellite denoted by $\mathcal{A}$. The initial conditions are rewritten as follows:

$$\boldsymbol{\alpha}_{\mathcal{D}}(t_0) = \boldsymbol{\alpha}_{\mathcal{A}}(t_0) + \begin{bmatrix}\mathbf{0}_{5\times1}\\ \Delta\Omega\end{bmatrix} \tag{7}$$

$$\boldsymbol{\alpha}_{\mathcal{A}}(t_0) = \boldsymbol{\alpha}_{\mathcal{C}}(t_0) + \int_{t_0}^{t_0+\Delta t} \dot{\boldsymbol{\alpha}}_{\mathcal{C}}\,\mathrm{d}t \tag{8}$$

Based on (4), the ballistic coefficients remain constant. Moreover, according to the assumed dynamic model, since neither the potential Φ nor the density ρ depend explicitly on time t, the dynamical system representing each satellite is autonomous, i.e. if $\boldsymbol{\Gamma} \triangleq [x\ y\ z\ \dot{x}\ \dot{y}\ \dot{z}]^T$, then

$$\dot{\boldsymbol{\Gamma}} = \mathbf{F}(\boldsymbol{\Gamma}) \tag{9}$$

where $\mathbf{F}$ is a vector-valued function. Therefore, if

$$\boldsymbol{\Gamma}_{\mathcal{A}}(t_0) = \boldsymbol{\Gamma}_{\mathcal{C}}(t_0 + \Delta t) = \boldsymbol{\Gamma}_{\mathcal{C}}(t_0) + \int_{t_0}^{t_0+\Delta t} \dot{\boldsymbol{\Gamma}}_{\mathcal{C}}\,\mathrm{d}t \tag{10}$$

then

$$\boldsymbol{\Gamma}_{\mathcal{A}}(t) = \boldsymbol{\Gamma}_{\mathcal{C}}(t + \Delta t) \tag{11}$$

Hence,

$$\|\mathbf{r}_{\mathcal{A}}(t) - \mathbf{r}_{\mathcal{C}}(t)\| = \|\mathbf{r}_{\mathcal{C}}(t + \Delta t) - \mathbf{r}_{\mathcal{C}}(t)\| < V_{\max}\,|\Delta t| \tag{12}$$

Next, the distance between the satellites $\mathcal{D}$ and $\mathcal{A}$ will be analyzed. The initial conditions selected for $\mathcal{D}$ and $\mathcal{A}$ can be explicitly stated as $a_{\mathcal{A}}(t_0) = a_{\mathcal{D}}(t_0)$, $e_{\mathcal{A}}(t_0) = e_{\mathcal{D}}(t_0)$, $i_{\mathcal{A}}(t_0) = i_{\mathcal{D}}(t_0)$, $\omega_{\mathcal{A}}(t_0) = \omega_{\mathcal{D}}(t_0)$, $f_{\mathcal{A}}(t_0) = f_{\mathcal{D}}(t_0)$, $\Omega_{\mathcal{A}}(t_0) + \Delta\Omega = \Omega_{\mathcal{D}}(t_0)$. Examining the GVE including drag and zonal harmonics,[17] it will next be shown that the resulting variational equations do not explicitly depend on Ω and thus the solutions of these equations are invariant with respect to a shift in the initial Ω. Consequently, $a_{\mathcal{A}}(t) = a_{\mathcal{D}}(t)$, $e_{\mathcal{A}}(t) = e_{\mathcal{D}}(t)$, $i_{\mathcal{A}}(t) = i_{\mathcal{D}}(t)$, $\omega_{\mathcal{A}}(t) = \omega_{\mathcal{D}}(t)$, $f_{\mathcal{A}}(t) = f_{\mathcal{D}}(t)$, $\Omega_{\mathcal{A}}(t) + \Delta\Omega = \Omega_{\mathcal{D}}(t)$.

The vector $\dot{\boldsymbol{\alpha}} = [\mathrm{d}a/\mathrm{d}t,\ \mathrm{d}e/\mathrm{d}t,\ \mathrm{d}i/\mathrm{d}t,\ \mathrm{d}\omega/\mathrm{d}t,\ \mathrm{d}f/\mathrm{d}t,\ \mathrm{d}\Omega/\mathrm{d}t]^T$ will be examined next. From the GVE, it is seen that Ω does not appear explicitly in the coefficients of the specific forces. Thus, to complete the proof it is necessary to show that none of the perturbing specific forces depend on Ω. To that end, the perturbing specific forces should be written in the LVLH frame. First, the specific forces due to the zonal harmonics are considered. The potential per unit mass of the zonal harmonics including the main gravitational term is

given in Eq. (1). The resulting acceleration can be expressed as follows:

$$-\mathbf{d}_J\Big|_{ECI} = \nabla\Phi = \begin{bmatrix} \frac{\partial\Phi}{\partial r}\frac{\partial r}{\partial x} \\ \frac{\partial\Phi}{\partial r}\frac{\partial r}{\partial y} \\ \frac{\partial\Phi}{\partial z} + \frac{\partial\Phi}{\partial r}\frac{\partial r}{\partial z} \end{bmatrix} \tag{13}$$

and therefore

$$\frac{\partial r}{\partial x} = \frac{x}{r} \qquad \frac{\partial r}{\partial y} = \frac{y}{r} \qquad \frac{\partial r}{\partial z} = \frac{z}{r} \tag{14}$$

Introducing the orbital elements, the expression in (14) can be re-written as[18]

$$\frac{\partial r}{\partial x} = c_{f+\omega}\, c_\Omega - c_i\, s_{f+\omega}\, s_\Omega \qquad \frac{\partial r}{\partial y} = c_{f+\omega}\, s_\Omega + c_i\, s_{f+\omega}\, c_\Omega \qquad \frac{\partial r}{\partial z} = s_i\, s_{f+\omega} \tag{15}$$

where c_ν and s_ν denote $\cos\nu$ and $\sin\nu$, respectively. In Eq. (13), the vector $\mathbf{d}_J$ is resolved in the ECI frame. To transform it into the LVLH frame, it is multiplied by the directional cosines matrix transforming any vector from ECI into LVLH. This matrix is termed D_{ECI}^{LVLH} and is given by:

$$D_{ECI}^{LVLH} = \begin{bmatrix} c_\Omega\, c_{\omega+f} - s_\Omega\, s_{\omega+f}\, c_i & s_\Omega\, c_{\omega+f} + c_\Omega\, s_{\omega+f}\, c_i & s_{\omega+f}\, s_i \\ -c_\Omega\, s_{\omega+f} - s_\Omega\, c_{\omega+f}\, c_i & -s_\Omega\, s_{\omega+f} + c_\Omega\, c_{\omega+f}\, c_i & c_{\omega+f}\, s_i \\ s_\Omega\, s_i & -c_\Omega\, s_i & c_i \end{bmatrix} \tag{16}$$

Hence,

$$-\mathbf{d}_J\Big|_{LVLH} = -D_{ECI}^{LVLH}\mathbf{d}_J\Big|_{ECI} = \begin{bmatrix} \frac{\partial\Phi}{\partial r} + s_{\omega+f}s_i\frac{\partial\Phi}{\partial z} \\ c_{\omega+f}s_i\frac{\partial\Phi}{\partial z} \\ c_i\frac{\partial\Phi}{\partial z} \end{bmatrix} \tag{17}$$

Since Φ is a scalar function of r and z, where

$$r = \frac{a(1-e^2)}{1 + e\, c_f} \tag{18}$$

and

$$z = r\, s_i\, s_{\omega+f} \tag{19}$$

the terms $\partial\Phi/\partial r$ and $\partial\Phi/\partial z$ can be functions of a, e, i, ω, and f but not of Ω. Consequently, $\mathbf{d}_J\Big|_{LVLH}$ does not depend on Ω.

To continue the analysis, the specific forces due to drag are considered. The acceleration generated by the atmospheric drag force can be modeled as in Eq. (2). In order to express

$\mathbf{d}_{Dr}$ in the LVLH frame, the vectors $\mathbf{v}$ and $\mathbf{v}_{atm}$ are multiplied by D_{ECI}^{LVLH}, and the following expressions are obtained:

$$(\mathbf{v}-\mathbf{v}_{atm})\Big|_{LVLH} = \begin{bmatrix} -e\left(c_{\omega+f}s_{\omega} - s_{\omega+f}c_{\omega}\right) \\ 1 + s_{\omega+f}es_{\omega} + c_{\omega+f}ec_{\omega} - \Psi_E s_i \\ s_i\Psi_E c_{\omega+f} \end{bmatrix} \tag{20}$$

The expression in Eq. (20) does not depend on Ω. Therefore, assuming a model of atmospheric density which is axially-symmetric with respect to the Earth's polar axis, i.e. $\rho(r,z) = \rho(a,e,i,\omega,f)$, it is concluded that $\mathbf{d}_{Dr}\Big|_{LVLH}$ is independent of Ω.

Since the solutions of the GVE with drag and zonal harmonics for the satellites $\mathcal{A}$ and $\mathcal{D}$ render all the orbital elements except Ω equal, the orbits of $\mathcal{A}$ and $\mathcal{D}$ are identical except the constant RAAN difference $\Delta\Omega$. This implies that $\eta_{\mathcal{A}} = \eta_{\mathcal{D}}$, and hence, based on the geometry shown in Fig. 1 and a straightforward application of the law of cosines, the distance between these two satellites is given by:

$$\|\mathbf{r}_{\mathcal{A}}(t) - \mathbf{r}_{\mathcal{D}}(t)\| = 2\sqrt{x_{\mathcal{A}}^2 + y_{\mathcal{A}}^2}\,\sin\left(\frac{|\Delta\Omega|}{2}\right) \tag{21}$$

Recalling that $\eta \triangleq \sqrt{x^2+y^2}$, the distance between the satellites $\mathcal{A}$ and $\mathcal{D}$ will always satisfy:

$$\|\mathbf{r}_{\mathcal{A}}(t) - \mathbf{r}_{\mathcal{D}}(t)\| \leq 2\,\eta_{\max}\,\sin\left(\frac{|\Delta\Omega|}{2}\right) \tag{22}$$

Applying the triangle inequality,

$$\|\mathbf{r}_{\mathcal{D}}(t) - \mathbf{r}_{\mathcal{C}}(t)\| \leq \|\mathbf{r}_{\mathcal{D}}(t) - \mathbf{r}_{\mathcal{A}}(t)\| + \|\mathbf{r}_{\mathcal{A}}(t) - \mathbf{r}_{\mathcal{C}}(t)\| < 2\,\eta_{\max}\,\sin\left(\frac{|\Delta\Omega|}{2}\right) + V_{\max}\,|\Delta t| \tag{23}$$

■

To proceed, denote some given reference orbit by $\boldsymbol{\alpha}_{[0;0]}(t_0)$. An orbit whose initial state is obtained through Eq. (5) is denoted by $\boldsymbol{\alpha}_{[\Delta\Omega;\Delta t]}(t_0)$. As a corollary of Proposition 1, different combinations of $\Delta\Omega$ and Δt will give infinite relative initial conditions that yield distance-bounded natural orbits for fractionated spacecraft, under the aforementioned assumptions. Assuming that the reference orbit is known, for a cluster comprised of more than two modules, some Δt and $\Delta\Omega$ can be assigned to each module, thus rendering distance-bounded motion among all the modules in the cluster. The values of Δt and $\Delta\Omega$ should be set according to the maximal allowed distance, $D_{\max}$, so that

$$|\Delta t|\,V_{\max} + 2\,\eta_{\max}\,\sin\left(\frac{|\Delta\Omega|}{2}\right) \leq D_{\max} \tag{24}$$

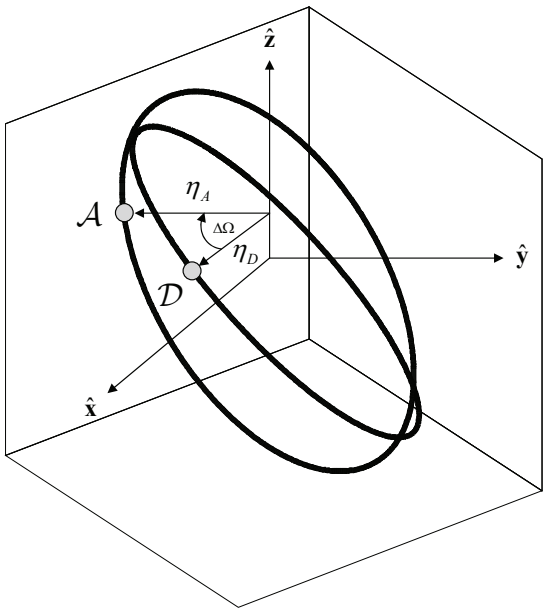

Figure 1. The geometry of two identical orbits with a differential RAAN, $\Delta\Omega$

Although the previous analysis considered only zonal harmonics and drag, simulations are shown in the sequel, in which other effects are added, namely sectorial and tesseral harmonics, solar radiation pressure and the lunisolar attraction. It will be shown that satellites satisfying the constraint given by Eq. (5) still exhibit a satisfactory behavior in terms of relative distance. Moreover, an example of a cluster with slightly different ballistic coefficients will be provided, showing that different ballistic coefficients can generate very large distances in short times. Therefore, for overcoming drag effects, it is important to keep small differences in the ballistic coefficients.

Since modules of fractionated spacecraft can be launched and released together, they should maneuver to attain initial conditions that satisfy Eq. (5). The next section presents an algorithm for cluster establishment.

CLUSTER ESTABLISHMENT USING IMPULSIVE MANEUVERS

It is imperative to design strategies to deploy the cluster, enabling each module to autonomously attain desired initial conditions once released by the launcher. The desired initial conditions for the modules are defined according to the mission specification, and the initial establishment maneuvers will be therefore inherently related to the state of each module immediately after the release.

This section presents a cluster establishment algorithm that enables two modules, $\mathcal{C}$ and $\mathcal{D}$, released at the same time from the same launcher, to reach desired initial conditions with

respect to a nominal desired orbit. Moreover, relative initial conditions are determined so as to keep the distance between the modules below a given threshold for relatively long time intervals.

In order to extend the module lifetime as much as possible, it is necessary to search for maneuvers that utilize minimum fuel. The following algorithm assumes that each module is capable of exerting impulsive thrust along three orthogonal axes. Consequently, it is assumed that the fuel mass flow $\dot{m}$ is proportional to the 1-norm of the applied thrust $\mathbf{T}$, i.e.

$$\dot{m} = \frac{\|\mathbf{T}\|_1}{I_{sp}\, g_0}$$

where I_{sp} is the specific impulse of the engine and g_0 is the standard gravity acceleration at sea level.[19]

If the modules are released from the same launcher at the same time, immediately after the release the positions are practically the same, while slight differences may arise in the velocity vectors due to the release mechanisms. Moreover, due to launch accuracy limitations, the resulting orbital elements of the the modules may slightly differ from the nominal orbital elements required for the mission. Therefore, it is necessary to execute maneuvers aimed at: (i) yielding orbital elements within the tolerances given for the mission, and (ii) attaining relative initial conditions for keeping the distances among the modules below some given threshold. In the subsequent developments, the time immediately after the release will be denoted by t_i.

A nominal orbit is given in terms of a semimajor axis a_n, eccentricity e_n, inclination i_n , and argument of perigee ω_n. Moreover, tolerances that state the largest acceptable difference between the actual orbital elements and the nominal ones are given as well. These tolerances are denoted by ε_a, ε_e, ε_i, ε_ω, respectively. There is no reference to a nominal true anomaly because it evolves rapidly and periodically, nor to a nominal RAAN because the Earth's rotation causes a periodic behavior of the relative longitude between any point on the Earth's surface and the RAAN.

Since the modules forming a cluster are close to one another, it is reasonable to assume that if the orbital elements of $\mathcal{C}$ satisfy

$$|a_{\mathcal{C}} - a_n| \leq \varepsilon_a \tag{25}$$

$$|e_{\mathcal{C}} - e_n| \leq \varepsilon_e \tag{26}$$

$$|i_{\mathcal{C}} - i_n| \leq \varepsilon_i \tag{27}$$

$$|\omega_{\mathcal{C}} - \omega_n| \leq \varepsilon_\omega \tag{28}$$

then the orbital elements of $\mathcal{D}$ will be relatively close to the nominal ones as well.

In order to maintain operational distances among the modules for long time intervals, the established initial conditions should satisfy the constraint (5), with a suitable Δt and

$\Delta\Omega$. Denote by t_0 the time at the end of the establishment maneuver of satellite $\mathcal{C}$. The constraint (5) may be approximately satisfied by requiring that

$$a_{\mathcal{D}}^{+}(t_0 - \Delta t) = a_{\mathcal{C}}^{+}(t_0) \tag{29}$$

$$e_{\mathcal{D}}^{+}(t_0 - \Delta t) = e_{\mathcal{C}}^{+}(t_0) \tag{30}$$

$$i_{\mathcal{D}}^{+}(t_i) = i_{\mathcal{C}}^{+}(t_i) \tag{31}$$

$$\omega_{\mathcal{D}}^{+}(t_0 - \Delta t) = \omega_{\mathcal{C}}^{+}(t_0) \tag{32}$$

$$f_{\mathcal{D}}^{+}(t_0 - \Delta t) = f_{\mathcal{C}}^{+}(t_0) \tag{33}$$

$$\Omega_{\mathcal{D}}^{+}(t_i) = \Omega_{\mathcal{C}}^{+}(t_i) + \Delta\Omega \tag{34}$$

where the superscripts $(\cdot)^+$ and $(\cdot)^-$ indicate values of the corresponding orbital element after and before the corresponding velocity impulse. The condition established for the inclination i in Eqs. (31) is justified as the variation of $\Delta i \triangleq i_{\mathcal{D}} - i_{\mathcal{C}}$ due to perturbations along an interval of time $t_0 - t_i$ (which is of the order of magnitude of a single orbital period, as will be seen in the sequel) is negligible for the purpose of this algorithm.

The developed strategy intends to minimize the total $\|\mathbf{\Delta V}\|_1$ utilized by the collective maneuver. The collective maneuver consists of two velocity impulses executed by each satellite. At time $t = t_i$ both satellites execute a first velocity impulse. Later, satellite $\mathcal{C}$ performs its second velocity impulse at time $t = t_0 > t_i$, and $\mathcal{D}$ performs it at a time $t = t_0 - \Delta t > t_i$. These impulses are resolved in the respective LVLH frame $(\hat{r}, \hat{\theta}, \hat{h})$ of each satellite. For both satellites, the first velocity impulse causes a velocity change in all three axes, $\mathbf{\Delta V}_{\mathcal{C}_1} = \begin{bmatrix}\Delta V_{r_{\mathcal{C}_1}} & \Delta V_{\theta_{\mathcal{C}_1}} & \Delta V_{h_{\mathcal{C}}}\end{bmatrix}^T$ and $\mathbf{\Delta V}_{\mathcal{D}_1} = \begin{bmatrix}\Delta V_{r_{\mathcal{D}_1}} & \Delta V_{\theta_{\mathcal{D}_1}} & \Delta V_{h_{\mathcal{D}}}\end{bmatrix}^T$. The second impulses generate a velocity changes in the radial and along-track directions only, and are given by $\mathbf{\Delta V}_{\mathcal{C}_2} = \begin{bmatrix}\Delta V_{r_{\mathcal{C}_2}} & \Delta V_{\theta_{\mathcal{C}_2}} & 0\end{bmatrix}^T$ and $\mathbf{\Delta V}_{\mathcal{D}_2} = \begin{bmatrix}\Delta V_{r_{\mathcal{D}_2}} & \Delta V_{\theta_{\mathcal{D}_2}} & 0\end{bmatrix}^T$. The corresponding time between the impulses will be computed in the sequel.

The out-of-plane components of the first velocity impulses, $\Delta V_{h_{\mathcal{C}}}$ and $\Delta V_{h_{\mathcal{D}}}$, are aimed at satisfying Eq. (31). Since the modules are launched together, with resulting small differences between their orbital elements, it is expected that the resulting $\Delta\Omega$ will still satisfy inequality (24). In case it does not, a new correction impulse can be added at the points where $\omega + f = \pi/2$ or $\omega + f = 3\,\pi/2$.

According to the impulsive approximation of the GVE, $\Delta V_{h_{\mathcal{C}}}$ and $\Delta V_{h_{\mathcal{D}}}$ must satisfy:

$$\Delta V_{h_{\mathcal{D}}} = \frac{h_{\mathcal{D}}^{-}(t_i)}{r_{\mathcal{D}}^{-}(t_i)\,\cos\left(\theta_{\mathcal{D}}^{-}(t_i)\right)}\left[i_{\mathcal{C}}^{-}(t_i) - i_{\mathcal{D}}^{-}(t_i) + \frac{r_{\mathcal{C}}^{-}(t_i)\,\cos\left(\theta_{\mathcal{C}}^{-}(t_i)\right)}{h_{\mathcal{C}}^{-}(t_i)}\Delta V_{h_{\mathcal{C}}}\right] \tag{35}$$

where $h = \sqrt{\mu\,a\,(1-e^2)}$, and $\theta = f + \omega$.

$\Delta V_{h_{\mathcal{C}}}$ affects $\Omega_{\mathcal{C}}$ and $\omega_{\mathcal{C}}$, and $\Delta V_{h_{\mathcal{D}}}$ affects $\Omega_{\mathcal{D}}$ and $\omega_{\mathcal{D}}$. As $\mathbf{\Delta V}_{\mathcal{C}_2}$ and $\mathbf{\Delta V}_{\mathcal{D}_2}$ do not contain out-of-plane components, they will vary neither the inclinations nor the RAANs. On the other hand, the in-plane components of the first and second impulses of both satellites

are aimed at attaining a, e, ω and f for $\mathcal{C}$ and $\mathcal{D}$ so as to satisfy Eqs. (25)-(26), (28)-(30), (32)-(33), by minimizing the consumed fuel.

To obtain $\Delta V_{r_{\mathcal{C}_1}}$, $\Delta V_{\theta_{\mathcal{C}_1}}$, $\Delta V_{r_{\mathcal{C}_2}}$, and $\Delta V_{\theta_{\mathcal{C}_2}}$, the result described in the Appendix A is used. The required inputs are $a_{\mathcal{C}}^-(t_i)$, $e_{\mathcal{C}}^-(t_i)$, $f_{\mathcal{C}}^-(t_i)$, $\tilde{\omega}_{\mathcal{C}}$, and $a_{\mathcal{C}}^+(t_0)$, $e_{\mathcal{C}}^+(t_0)$, $f_{\mathcal{C}}^+(t_0)$, $\omega_{\mathcal{C}}^+(t_0)$, where

$$\tilde{\omega}_{\mathcal{C}} = \omega_{\mathcal{C}}^-(t_i) - \frac{r_{\mathcal{C}}^-(t_i)\,\sin(\theta_{\mathcal{C}}^-(t_i))}{h_{\mathcal{C}}^-(t_i)\,\tan\left(i_{\mathcal{C}}^-(t_i)\right)}\Delta V_{h_{\mathcal{C}}} \tag{36}$$

Although the utilized transfer approach does not assume perturbations, considering that the transfer time $dt_{trans_{\mathcal{C}}}$ is not too long, the two-body problem scenario is a good approximation for the real situation. This will be validated by numerical examples.

Assuming that generally $a_{\mathcal{C}}^-(t_i) \neq a_{\mathcal{D}}^-(t_i)$, $e_{\mathcal{C}}^-(t_i) \neq e_{\mathcal{D}}^-(t_i)$, $\tilde{\omega}_{\mathcal{C}} \neq \tilde{\omega}_{\mathcal{D}}$, and $f_{\mathcal{C}}^-(t_i) \neq f_{\mathcal{D}}^-(t_i)$, the optimal transfer for $\mathcal{C}$ and $\mathcal{D}$ would take different times, i.e. $dt_{trans_{\mathcal{C}}} \neq dt_{trans_{\mathcal{D}}}$. However, in order to satisfy Eqs. (29), (30), (32), and (33) for some t_0, once dt_{trans} was obtained for one of the modules, the other must attain the desired values in a transfer time $dt_{trans} + \Delta t$. Therefore, if satellite $\mathcal{C}$ executes its optimal transfer, satellite $\mathcal{D}$ can attain the desired orbital elements in the desired time by making use of the Lambert problem solution.[20,17] Thus, solving the corresponding Lambert problem with inputs given by $a_{\mathcal{D}}(t_i)$, $e_{\mathcal{D}}(t_i)$, $f_{\mathcal{D}}(t_i)$, $\tilde{\omega}_{\mathcal{D}}$ as the initial state, a_f, e_f, f_f, ω_f as the final state, and an interval of time $dt_{trans} - \Delta t$, one determines the in-plane velocity impulses $\Delta V_{r_{\mathcal{D}_1}}$, $\Delta V_{\theta_{\mathcal{D}_1}}$ and $\Delta V_{r_{\mathcal{D}_2}}$, $\Delta V_{\theta_{\mathcal{D}_2}}$. Notice that if the differences between the orbital elements of $\mathcal{C}$ and $\mathcal{D}$ are small at $t = t_i$, and if Δt is also small, the Lambert solution would be close to that obtained by the co-planar optimal transfer.

There is another important constraint to establish for the collective maneuver of $\mathcal{C}$ and $\mathcal{D}$. The constraint stated in Eq. (5) assumed that $\mathcal{C}$ and $\mathcal{D}$ have identical ballistic coefficients. Since significant differences in the ballistic coefficients can cause large relative distances between the modules in a relatively short time, the collective maneuver should attempt to keep the difference between the ballistic coefficients within a given tolerance. This constraint is stated as

$$\left|\frac{C_{D_{\mathcal{D}}}S_{\mathcal{D}}}{m_{\mathcal{D}}} - \frac{C_{D_{\mathcal{C}}}S_{\mathcal{C}}}{m_{\mathcal{C}}}\right| \leq \varepsilon_m \tag{37}$$

As was previously mentioned, the maneuvers are planned to minimize fuel consumption. Therefore, the joint maneuver is seen as an optimization problem of the form

$$\min_{\boldsymbol{\beta}} \Delta V_{tot} = \min_{\boldsymbol{\beta}} \left[\|\boldsymbol{\Delta \mathbf{V}}_{\mathcal{C}_1}\|_1 + \|\boldsymbol{\Delta \mathbf{V}}_{\mathcal{C}_2}\|_1 + \|\boldsymbol{\Delta \mathbf{V}}_{\mathcal{D}_1}\|_1 + \|\boldsymbol{\Delta \mathbf{V}}_{\mathcal{D}_2}\|_1\right] \tag{38}$$

where $\boldsymbol{\beta} = \left\{\Delta V_{h_{\mathcal{C}}}\ a_{\mathcal{C}}^+(t_0), e_{\mathcal{C}}^+(t_0), \omega_{\mathcal{C}}^+(t_0), f_{\mathcal{C}}^+(t_0)\right\}$, subject to constraints (24), (25)-(28), and (37). Algorithm 1 summarizes the complete maneuver for the modules $\mathcal{C}$ and $\mathcal{D}$.

It is well-known that it is desirable to correct the inclination when the satellites are close to the equatorial plane. Therefore, this joint maneuver should be commenced when, after the release, the orbital elements of one of the satellites satisfies

$$|f(t_i) + \omega(t_i)| \leq \varepsilon_{init} \tag{39}$$

Algorithm 1 Algorithm for initial conditions establishment for cluster keeping

1: Given Initial Conditions, $\boldsymbol{\alpha}_{\mathcal{C}}^{-}(t_i)$ and $\boldsymbol{\alpha}_{\mathcal{D}}^{-}(t_i)$. Propose a Δt.
2: Determine $\Delta V_{h_{\mathcal{C}}}$, $a_{\mathcal{C}}^{+}(t_0)$, $e_{\mathcal{C}}^{+}(t_0)$, $\omega_{\mathcal{C}}^{+}(t_0)$, $f_{\mathcal{C}}^{+}(t_0)$, using an optimization algorithm.
3: **for** $\Delta V_{h_{\mathcal{C}}}$, $a_{\mathcal{C}}^{+}(t_0)$, $e_{\mathcal{C}}^{+}(t_0)$, $\omega_{\mathcal{C}}^{+}(t_0)$, $f_{\mathcal{C}}^{+}(t_0)$ **do**
4: Compute $\Delta V_{h_{\mathcal{D}}} = \frac{h_{\mathcal{D}}^{-}(t_i)}{r_{\mathcal{D}}^{-}(t_i)\,\cos\left(\theta_{\mathcal{D}}^{-}(t_i)\right)}\left[i_{\mathcal{C}}^{-}(t_i) + \frac{r_{\mathcal{C}}^{-}(t_i)\,\cos\left(\theta_{\mathcal{C}}^{-}(t_i)\right)}{h_{\mathcal{C}}^{-}(t_i)}\Delta V_{h_{\mathcal{C}}}\right]$. It yields after the first impulse, $i_{\mathcal{C}} = i_{\mathcal{D}} = \left[i_{\mathcal{C}}^{-}(t_i) + \frac{r_{\mathcal{C}}^{-}(t_i)\,\cos\left(\theta_{\mathcal{C}}^{-}(t_i)\right)}{h_{\mathcal{C}}^{-}(t_i)}\Delta V_{h_{\mathcal{C}}}\right]$.
5: Compute $\Delta\Omega = \Omega_{\mathcal{D}}^{+}(t_i) - \Omega_{\mathcal{C}}^{+}(t_i)$
6: Compute the respective arguments of perigee due to $\Delta V_{h_{\mathcal{C}}}$ and $\Delta V_{h_{\mathcal{D}}}$ as $\tilde{\omega}_{\mathcal{C}} = \omega_{\mathcal{C}}^{-}(t_i) - \frac{r_{\mathcal{C}}^{-}(t_i)\,\sin(\theta_{\mathcal{C}}^{-}(t_i))}{h_{\mathcal{C}}^{-}(t_i)\,\tan\left(i_{\mathcal{C}}^{-}(t_i)\right)}\Delta V_{h_{\mathcal{C}}}$ and $\tilde{\omega}_{\mathcal{D}} = \omega_{\mathcal{D}}^{-}(t_i) - \frac{r_{\mathcal{D}}^{-}(t_i)\,\sin(\theta_{\mathcal{D}}^{-}(t_i))}{h_{\mathcal{D}}^{-}(t_i)\,\tan\left(i_{\mathcal{D}}^{-}(t_i)\right)}\Delta V_{h_{\mathcal{D}}}$
7: With $\left[a_{\mathcal{C}}^{-}(t_i),\, e_{\mathcal{C}}^{-}(t_i),\, f_{\mathcal{C}}^{-}(t_i),\, \tilde{\omega}_{\mathcal{C}}\right]$ as initial state and $\left[a_{\mathcal{C}}^{+}(t_0),\, e_{\mathcal{C}}^{+}(t_0),\, f_{\mathcal{C}}^{+}(t_0),\, \omega_{\mathcal{C}}^{+}(t_0)\right]$ solve the co-planar two-impulse optimal transfer (according to Appendix 1), obtain the respective transfer time dt_{trans}, and $t_0 = t_i + dt_{trans}$.
8: Obtain the required satellite $\mathcal{C}$ velocity changes, in the corresponding LVLH frames. The vectors $\boldsymbol{\Delta}\mathbf{V}$ for the first and second impulse of the satellite $\mathcal{C}$ are denoted as: $\boldsymbol{\Delta}\mathbf{V}_{\mathcal{C}_1} = \left[\Delta V_{r_{\mathcal{C}_1}}\ \Delta V_{\theta_{\mathcal{C}_1}}\ \Delta V_{h_{\mathcal{C}}}\right]^T$ and $\boldsymbol{\Delta}\mathbf{V}_{\mathcal{C}_2} = \left[\Delta V_{r_{\mathcal{C}_2}}\ \Delta V_{\theta_{\mathcal{C}_2}}\ 0\right]^T$.
9: Define $a_{\mathcal{D}}^{+}(t_0 - \Delta t) = a_{\mathcal{C}}^{+}(t_0)$, $e_{\mathcal{D}}^{+}(t_0 - \Delta t) = e_{\mathcal{C}}^{+}(t_0)$, $\omega_{\mathcal{D}}^{+}(t_0 - \Delta t) = \omega_{\mathcal{C}}^{+}(t_0)$, $f_{\mathcal{D}}^{+}(t_0 - \Delta t) = f_{\mathcal{C}}^{+}(t_0)$
10: With $\left[a_{\mathcal{D}}^{-}(t_i),\, e_{\mathcal{D}}^{-}(t_i),\, f_{\mathcal{D}}^{-}(t_i),\, \tilde{\omega}_{\mathcal{D}}\right]$ as initial state and $\left[a_{\mathcal{D}}^{+}(t_0 - \Delta t),\ e_{\mathcal{D}}^{+}(t_0 - \Delta t),\ \omega_{\mathcal{D}}^{+}(t_0 - \Delta t),\ f_{\mathcal{D}}^{+}(t_0 - \Delta t)\right]$, and with an interval of time $dt_{trans} - \Delta t$, solve the corresponding Lambert Problem.
11: Obtain the required velocity changes for satellite $\mathcal{D}$, in the corresponding LVLH frames. The vectors $\boldsymbol{\Delta}\mathbf{V}$ for the first and second impulse of the satellite $\mathcal{D}$ are denoted as: $\boldsymbol{\Delta}\mathbf{V}_{\mathcal{D}_1} = \left[\Delta V_{r_{\mathcal{D}_1}}\ \Delta V_{\theta_{\mathcal{D}_1}}\ \Delta V_{h_{\mathcal{D}}}\right]^T$ and $\boldsymbol{\Delta}\mathbf{V}_{\mathcal{D}_2} = \left[\Delta V_{r_{\mathcal{D}_2}}\ \Delta V_{\theta_{\mathcal{D}_2}}\ 0\right]^T$.
12: Compute the total cost of the maneuver as $\Delta V_{tot} = \|\boldsymbol{\Delta}\mathbf{V}_{\mathcal{C}_1}\|_1 + \|\boldsymbol{\Delta}\mathbf{V}_{\mathcal{C}_2}\|_1 + \|\boldsymbol{\Delta}\mathbf{V}_{\mathcal{D}_1}\|_1 + \|\boldsymbol{\Delta}\mathbf{V}_{\mathcal{D}_2}\|_1$
13: Evaluate the constraints given by inequalities (24), (25)-(28), and (37).
14: **end for**
15: GOTO 2

If upon the release none of the modules satisfies the constraint given in (39), the maneuver will start only when at least one of them satisfies it.

NUMERICAL RESULTS

Calculation of initial conditions

The following examples illustrates the use of Eq. (5) to find relative initial conditions that yield natural long-term distance-bounded orbits. The first example assumes zonal harmonics up to degree $n = 21$ and drag according to the ISA-1976 model. It is assumed that a maximal distance between the modules of $D_{\max} = 2$ km is allowed. For this case, the modules have the following parameters: $m_{\mathcal{C}} = m_{\mathcal{D}} = 35$ kg, $C_{D_{\mathcal{C}}} = C_{D_{\mathcal{D}}} = 2.2$, and $S_{\mathcal{C}} = S_{\mathcal{C}} = 0.35$ m^2. A reference orbit is defined by the following initial conditions:

$$\boldsymbol{\alpha}_{\mathcal{C}}(t_0) = \left[7500 \text{ km},\ 0.1,\ 35^\circ,\ 0^\circ,\ 0^\circ,\ 0^\circ\right]^T \tag{40}$$

For this reference orbit, $V_{\max} = 8.061$ km/sec and $\eta_{\max} = 8228.6$ km. Thus, setting, for instance, $\Delta\Omega = 0.00418^\circ$ and $\Delta t = 0.1$ sec yields $|\Delta t|\, V_{\max} + 2\,\eta_{\max} \sin\left(|\Delta\Omega|/2\right) = 1.4065$ km $< D_{\max}$. According to Eq. (5), the initial conditions for a module $\mathcal{D}$ are obtained as $\boldsymbol{\alpha}_{\mathcal{D}}(t_0) = [7499.999992323$ km; 0.099999999; 34.999999972°; 0.000099452°; 0.006741747°; $0.00418^\circ]^T$. The distances between the satellites is shown in Fig. 2, and designated as Case I. It is seen that according to the bound (24), the distance between the satellites always remains below $D_{\max}$.

With the vectors $\boldsymbol{\alpha}_{\mathcal{C}}(t_0)$ and $\boldsymbol{\alpha}_{\mathcal{D}}(t_0)$ and the same satellite parameters, another simulation was performed while adding other perturbations to the model. The added perturbations include lunisolar attraction, sectorial and tesseral harmonics, solar radiation pressure, tides, and relativistic corrections. Moreover, the atmospheric density was specified according to the Jacchia-Roberts model,[17] which includes variations due to seasons, latitude, and local time. The resulting distance is also shown in Fig. 2, and designated as Case II. As the perturbations considered in this simulation depend explicitly on t and Ω, as opposed to the conditions leading to Proposition 1, it is expected that the distance between the satellites goes beyond the bound (24). However, the distance still remains below $D_{\max}$ and is therefore still operational for more than 60 days – without any maneuvers.

Finally, with the same initial conditions and the added perturbations, a new simulation was conducted, but the mass of $\mathcal{D}$ was modified to $m_{\mathcal{D}} = 34.5$ kg, which is equivalent to varying the ballistic coefficient. The distance for this case is plotted in Fig. 3. It is seen that the relative distance is strongly affected by the difference between ballistic coefficients. This justifies the importance of satisfying the constraint (37).

Establishment Algorithm Implementation

This section shows an example, in which the modules are required to stay within about $D_{\max} = 3$ km. The initial conditions after the release are randomly generated by using a Gaussian distribution. The respective means are established by the nominal initial conditions given as $\boldsymbol{\alpha}_n = [7500\,\text{km},\ 0.1,\ 30^\circ,\ 0^\circ,\ 0^\circ,\ 0^\circ]^T$, and the standard deviations are

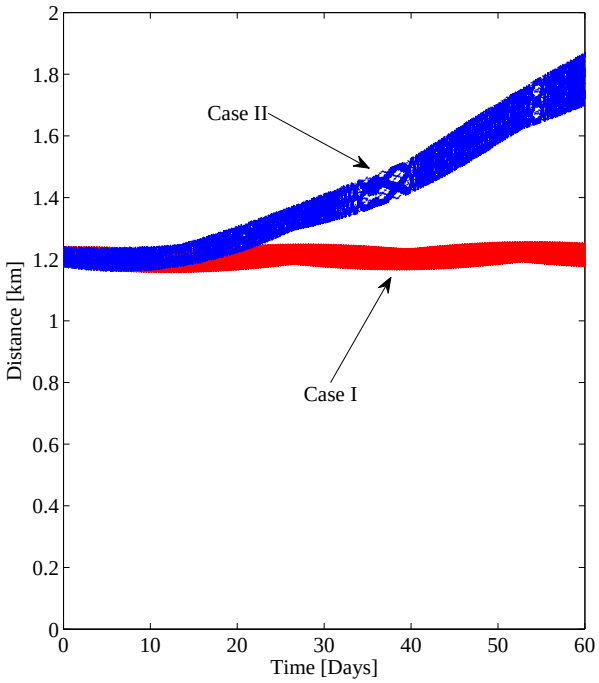

Figure 2. Distance between satellites $\mathcal{C}$ and $\mathcal{D}$

$\sigma_{\mathbf{r}} = 4/3$ km for every position component, and $\sigma_{\mathbf{v}} = 0.67$ m/sec for every velocity component. As previously noted, the position vectors after the release are the same for both satellites, while the velocity vectors are different. The obtained initial conditions immediately after the release, are given by

$$\mathbf{r}_{\mathcal{C}}^{-}(t_i) = \mathbf{r}_{\mathcal{D}}^{-}(t_i) = \begin{bmatrix} 6750.063866 \\ 0.019343 \\ -0.572880 \end{bmatrix} \text{ km}$$

$$\mathbf{v}_{\mathcal{C}}^{-}(t_i) = \begin{bmatrix} 0.000084 \\ 6.980008 \\ 4.029034 \end{bmatrix} \text{ km/sec} \qquad \mathbf{v}_{\mathcal{D}}^{-}(t_i) = \begin{bmatrix} 0.000794 \\ 6.980609 \\ 4.029774 \end{bmatrix} \text{ km/sec}$$

The initial masses of the satellites are given by $m_{\mathcal{C}} = m_{\mathcal{D}} = 35$ kg. The drag coefficients of both satellites are taken as $C_{D_{\mathcal{C}}} = C_{D_{\mathcal{D}}} = 2.2$ and the cross-sectional area of the satellites are $S_{\mathcal{C}} = S_{\mathcal{D}} = 0.071\ m^2$. The specific impulse of the thrusters is $I_{sp} = 200$ sec. The

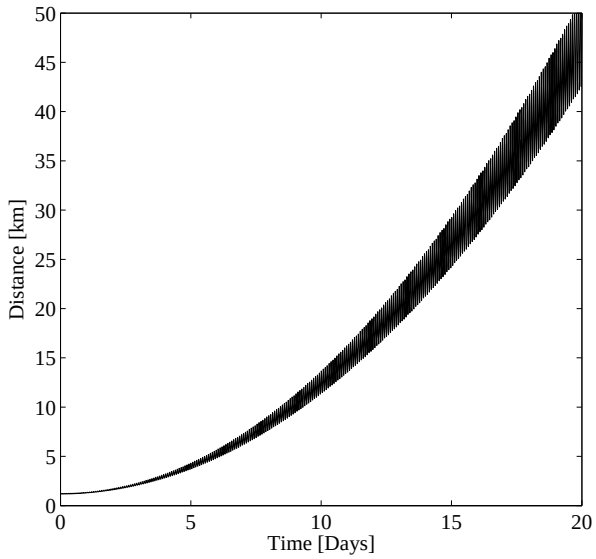

Figure 3. Distance between satellites $\mathcal{C}$ and $\mathcal{D}$, for different ballistic coefficients

initial orbital elements of both modules are given by:

$$\boldsymbol{\alpha}_{\mathcal{C}}^{-}(t_i)(= \begin{bmatrix} 7499.6664\,\text{km} \\ 0.09995 \\ 29.9946^\circ \\ 0.00892^\circ \\ 359.9813^\circ \\ 0.00859^\circ \end{bmatrix} \qquad \boldsymbol{\alpha}_{\mathcal{D}}^{-}(t_i) = \begin{bmatrix} 7501.6915\,\text{km} \\ 0.10019 \\ 29.9970^\circ \\ -0.04656^\circ \\ 0.0368^\circ \\ 0.00859^\circ \end{bmatrix}$$

The tolerances for the mission were set as $\varepsilon_a = 0.5\,\text{km}$, $\varepsilon_e = 5 \times 10^{-3}$, $\varepsilon_i = 0.5^\circ$, $\varepsilon_\omega = 5^\circ$, and $\varepsilon_m = 1.25 \times 10^{-5}\,\text{m}^2/\text{kg}$. If no maneuvers were performed, the distance between the satellites would increase as shown in Figure 4. After 25 minutes the distance between the modules exceeds 3 km, which is not satisfactory for the mission. For this case, the algorithm was executed with a $\Delta t = -0.1$sec. The other parameters necessary to evaluate the constraint are $V_{\max} = 8.062\,\text{km/sec}$ and $\eta_{\max} = 8231.77\,\text{km}$, which are evaluated based on the nominal orbit data. The obtained maneuver for the module $\mathcal{C}$ is as follows: At time $t = t_i$ a velocity impulse of $\boldsymbol{\Delta V}_{\mathcal{C}_1} = [-10.397\ 0.865\ 0.211]^T$m/sec in the respective LVLH frame is applied. Then the satellite continues its trajectory for an interval of $dt_{trans_{\mathcal{C}}} = 4329.39$ seconds, where a new velocity impulse is applied as $\boldsymbol{\Delta V}_{\mathcal{C}_2} = [-10^{-12}\ \ -1.098\ 0]^T$m/sec in the corresponding LVLH frame. The maneuver for the module $\mathcal{D}$ is as follows: at time $t = t_i$ a velocity impulse of $\boldsymbol{\Delta V}_{\mathcal{D}_1} = [-11.015\ \ -7.403 \times 10^{-9}\ \ -0.129]^T$m/sec in the respective LVLH frame is applied. Then the satellite continues its trajectory for an interval of $dt_{trans_{\mathcal{D}}} = 4329.49$ seconds, where a new velocity impulse is applied as $\boldsymbol{\Delta V}_{\mathcal{D}_2} = [0.094\ -1.119\ 0]^T$m/sec in the corresponding LVLH frame. After performing the two respective impulses, the final masses

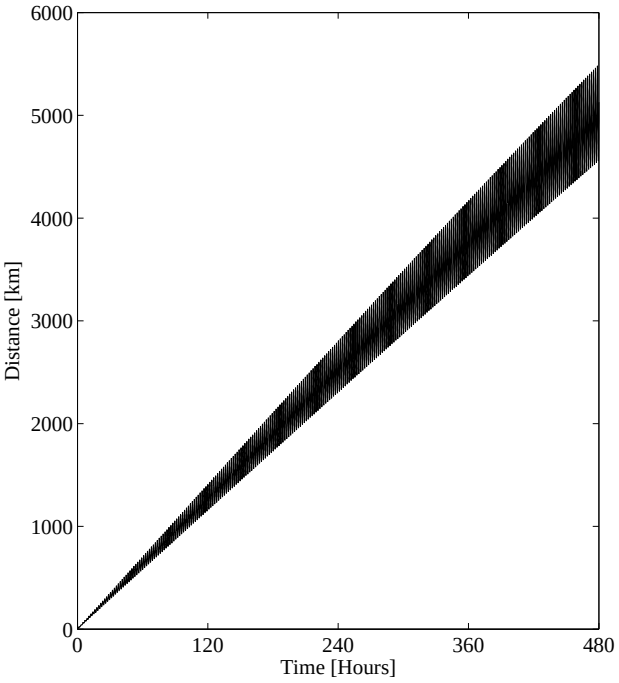

Figure 4. Distance between satellites $\mathcal{C}$ and $\mathcal{D}$ if no maneuver is performed.

of both satellites are $m_{\mathcal{C}} = 34.7764\,\text{kg}$ and $m_{\mathcal{D}} = 34.7802\,\text{kg}$. The obtained relative distances are illustrated in Fig. 5. As previously mentioned, the transfer times $dt_{trans_{\mathcal{C}}}$ and $dt_{trans_{\mathcal{D}}}$ are of the order of magnitude of 1 orbital period. The orbital elements obtained from the algorithm are as follows: $a_{\mathcal{C}}^{+}(t_0) = a_{\mathcal{D}}^{+}(t_0 - \Delta t) = 7499.5233\,\text{km}$, $e_{\mathcal{C}}^{+}(t_0) = e_{\mathcal{D}}^{+}(t_0 - \Delta t) = 0.1004$, $i_{\mathcal{C}}^{+}(t_i) = i_{\mathcal{D}}^{+}(t_i) = 29.996°$, $\omega_{\mathcal{C}}^{+}(t_0) = \omega_{\mathcal{D}}^{+}(t_0 - \Delta t) = 0.9579°$, $f_{\mathcal{C}}^{+}(t_0) = f_{\mathcal{D}}^{+}(t_0 - \Delta t) = 230.87°$, $\Omega_{\mathcal{C}}^{+}(t_i) = 0.00859°$, and $\Omega_{\mathcal{D}}^{+}(t_i) = 0.00859°$. Although $\Omega_{\mathcal{C}}^{+}(t_i)$ and $\Omega_{\mathcal{D}}^{+}(t_i)$ appear to be the same, and consequently the modules seem to be in the same orbital plane, there is a slight difference between the RAANs. For this specific case, the resulting difference between $\Omega_{\mathcal{C}}^{+}(t_i)$ and $\Omega_{\mathcal{D}}^{+}(t_i)$ is particularly small due to the initial conditions. However, generally a larger difference between the RAANs is obtained, but still satisfying the required constraints. The total velocity correction obtained for this case is $\Delta V_{tot} = 24.93\,\text{m/sec}$.

The simulation illustrated in Fig. 5 includes zonal, sectorial and tesseral harmonics up to degree and order 21, drag with the density model of Jacchia-Roberts, lunisolar attraction, solar radiation pressure, tides and relativistic corrections, intending to represent a real space environment. Moreover, the simulation was performed with the corresponding ballistic coefficients, updated after each velocity impulse. The use of the described algorithm proves to be a useful approach for cluster establishment. It is seen that in an interval longer than 20 days, no other maneuver is required to maintain the relative distance below $D_{\max}$.

If the orbital elements of the satellites exceed the tolerances given for the mission, or the

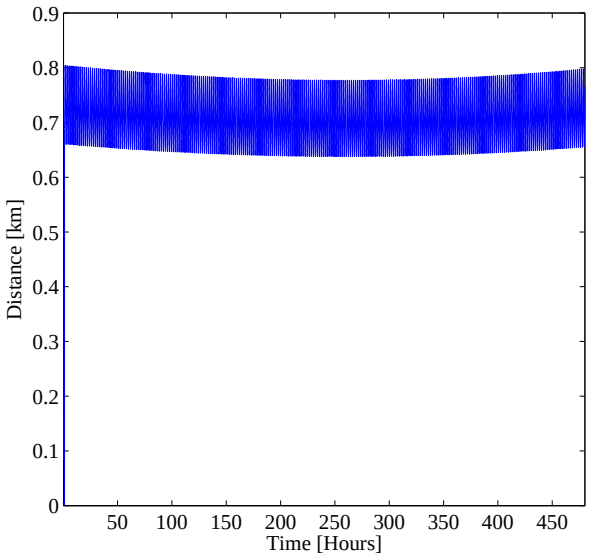

Figure 5. Distance between satellites $\mathcal{C}$ and $\mathcal{D}$ when the cluster establishment algorithm is applied.

distance between the modules reaches some upper limit (as seen in Fig. 4), the algorithm could be re-executed and a new maneuver would take place, such that all the necessary constraints are satisfied. Thus, the new cluster establishment algorithm can be straightforwardly used for cluster-keeping.

CONCLUSION

This paper presented a preliminary methodological study of cluster flight for fractionated spacecraft systems. To obtain distance-bounded relative motion between the cluster modules, a new constraint on the initial conditions of the modules was stated. A concomitant analytical bound on the relative distance between the modules was proven based on a design model assuming time-invariance of the environmental perturbations. Nevertheless, it was shown that if the actual astrodynamical model includes other, possibly time-varying effects, mild drifts between the modules can be obtained. Numerical simulations has shown that the relative distance between the modules, satisfying the mentioned constraint, is kept bounded for relatively long intervals of time.

Furthermore, this paper presented a cluster establishment algorithm for tracking a given nominal orbit, whose characteristics satisfy the previously-develop no-drift constraint. This algorithm is comprised of tools leading to fuel balancing among the maneuvering modules as well as minimization of the total fuel consumption. It was shown that properly balancing the fuel consumption is important no only for preventing some of the modules to run out of fuel, but also for keeping the ballistic coefficients similar, which is essential for fuel-efficient cluster-keeping. The same algorithm used for cluster establishment can also be used for cluster-keeping.

ACKNOWLEDGMENTS

This research was supported by the Technion Graduate Fellowships Program and by the Ministry of Science and Technology of the State of Israel.

APPENDIX A: OPTIMAL CO-PLANAR BI-IMPULSE ORBITAL TRANSFER

Consider a single satellite in a two-body problem setup. Assume that the initial a_0, e_0, ω_0 and f_0, and the final a_f, e_f, ω_f and f_f are given, and that the initial and final orbits are co-planar. The given orbital elements define the initial position and velocity vectors, $\mathbf{r}_0$, $\mathbf{v}_0$ respectively, and the corresponding final vectors, $\mathbf{r}_f$ and $\mathbf{v}_f$.

To find the impulses that yield the fuel-optimal two-impulse transfer, for a spacecraft equipped with three mutually orthogonal thrusters aligned with the LVLH frame, it is necessary to minimize the following function J, i.e.:

$$\begin{aligned}\min_{v_\rho} J &= \min_{v_\rho} \left(\|\mathbf{\Delta V}_1\|_1 + \|\mathbf{\Delta V}_2\|_1\right) \\ &= \min_{v_\rho} (|v_\rho - v_{\rho_0} + (v_c - v_{c_0})\,\cos\phi_1| + |(v_c - v_{c_0})\,\sin\phi_1| \\ &+ |v_{\rho_f} + v_\rho + (v_{c_f} - v_c)\,\cos\phi_2| + |(v_{c_f} - v_c)\,\sin\phi_2|)\end{aligned} \tag{41}$$

where:

- ϕ_1 is the angle between $\hat{\mathbf{r}}_0$ and $\hat{\mathbf{c}}$ measured counter-clockwise
- ϕ_2 is the angle between $\hat{\mathbf{r}}_f$ and $\hat{\mathbf{c}}$ measured counter-clockwise
- $\hat{\mathbf{r}}_0$ is a unit vector in the direction of the initial position vector, determined by a_0, e_0, ω_0 and f_0
- $\hat{\mathbf{r}}_f$ is a unit vector in the direction of the final position vector, determined by a_f, e_f, ω_f and f_f
- $\hat{\mathbf{c}} = \frac{\mathbf{r}_f - \mathbf{r}_0}{\|\mathbf{r}_f - \mathbf{r}_0\|}$
- $v_c = \frac{\alpha}{v_\rho}$
- $\alpha = \frac{c\,\mu}{r_0\,r_f}\frac{1-\cos\eta}{\sin^2\eta}$
- η is the angle between $\mathbf{r}_0$ and $\mathbf{r}_f$
- $c = \|\mathbf{r}_f - \mathbf{r}_0\|$
- $r_0 = \|\mathbf{r}_0\|$
- $r_f = \|\mathbf{r}_f\|$
- v_{r_0} and v_{c_0} are the respective coordinates of the velocity vector $\mathbf{v}_0$, resolved in a non-orthogonal basis given by the vectors $(\hat{\mathbf{r}}_0, \hat{\mathbf{c}})$

- v_{r_f} and v_{c_f} are the respective coordinates of the velocity vector $\mathbf{v}_f$, resolved in a non-orthogonal basis given by the vectors $(\hat{\mathbf{r}}_f, \hat{\mathbf{c}})$

The v_ρ that globally minimizes J is selected among the following candidates:

$$v_{\rho_1} = -\frac{1}{2}\sqrt{-2\cos(\phi_2)\,\alpha + 2\,\cos(\phi_1)\,\alpha + 2\alpha\sqrt{-\cos^2\phi_2 + \cos^2\phi_1 + 2\sin^2\phi_1 + 2\sin\phi_1\sin\phi_2}} \tag{42}$$

$$v_{\rho_{2,3}} = \begin{cases} \frac{1}{2}\left[\cos\phi_1\, v_{c0} + v_{\rho_0} + \sqrt{\cos^2\phi_1\, {v_{c_0}}^2 + 2\,\cos\phi_1\, v_{c_0} v_{\rho_0} + {v_{\rho_0}}^2 - 4\,\cos\phi_1\,\alpha}\right] \\ \frac{1}{2}\left[\cos\phi_1\, v_{c_0} + v_{\rho_0} - \sqrt{\cos^2\phi_1\, {v_{c_0}}^2 + 2\,\cos\phi_1\, v_{c_0} v_{\rho_0} + {v_{\rho_0}}^2 - 4\,\cos\phi_1\,\alpha}\right] \end{cases} \tag{43}$$

$$v_{\rho_4} = \frac{\alpha}{v_{c_0}} \tag{44}$$

$$v_{\rho_{5,6}} = \begin{cases} \frac{1}{2}\left[-\cos\phi_2\, v_{c_3} - v_{\rho_3} + \sqrt{\cos^2\phi_2\, {v_{c_3}}^2 + 2\,\cos\phi_2\, v_{c_3} v_{\rho_3} + {v_{\rho_3}}^2 + 4\,\cos\phi_2\,\alpha}\right] \\ \frac{1}{2}\left[-\cos\phi_2\, v_{c_3} - v_{\rho_3} - \sqrt{\cos^2\phi_2\, {v_{c_3}}^2 + 2\,\cos\phi_2\, v_{c_3} v_{\rho_3} + {v_{\rho_3}}^2 + 4\,\cos\phi_2\,\alpha}\right] \end{cases} \tag{45}$$

$$v_{\rho_7} = \frac{\alpha}{v_{c_3}} \tag{46}$$

By computing the seven candidates as functions of the given parameters, and evaluating J at each of them, one can choose the optimal v_ρ. Then, the corresponding velocity impulses are given by:

$$\begin{aligned} \mathbf{\Delta V}_1 &= \begin{bmatrix} \Delta V_{r_1} \\ \Delta V_{\theta_1} \end{bmatrix} = \begin{bmatrix} v_\rho - v_{\rho_0} + (v_c - v_{c_0})\,\cos\phi_1 \\ (v_c - v_{c_0})\,\sin\phi_1 \end{bmatrix} \\ \mathbf{\Delta V}_2 &= \begin{bmatrix} \Delta V_{r_2} \Delta V_{\theta_2} \end{bmatrix} = \begin{bmatrix} v_{\rho_f} + v_\rho + (v_{c_f} - v_c)\,\cos\phi_2 \\ (v_{c_f} - v_c)\,\sin\phi_2 \end{bmatrix} \end{aligned} \tag{47}$$

Once v_ρ is obtained, one can obtain the orbital elements of the transfer orbit, and by the Kepler equation determine the transfer time dt_{trans}.

REFERENCES

[1] O. Brown and P. Eremenko, "Fractionated Space Architectures: A Vision for Responsive Space," *4th Responsive Space Conference*, Los Angeles, CA, 2006.

[2] C. Mathieu and L. Weigel, "Assessing the Fractionated Spacecraft Concept," *Space 2006*, San Jose, CA, 2006.

[3] P. Gurfil, "Relative Motion Between Elliptic Orbits: Generalized Boundedness Conditions and Optimal Formationkeeping," *Journal of Guidance, Control, and Dynamics*, Vol. 28, July-August 2005, pp. 761–767.

[4] I. M. Ross, "Linearized Dynamic Equations for Spacecraft Subject to J_2 Perturbations," *Journal of Guidance, Control and Dynamics*, Vol. 26, May-June 2003, pp. 657–659.

[5] S. R. Vadali, "An Analytical Solution for Relative Motion of Satellites," *5th Dynamics and Control of Systems and Structures in Space Conference*, Cranfield, UK, Cranfield University, July 2002.

[6] S. A. Schweighart and R. J. Sedwick, "High-Fidelity Linearized J_2 Model for Satellite Formation Flight," *Journal of Guidance, Control and Dynamics*, Vol. 25, No. 6, 2002, pp. 1073–1080.

[7] D.-W. Gim and K. T. Alfriend, "State Transition Matrix of Relative Motion for the Perturbed Noncircular Reference Orbit," *Journal of Guidance, Control, and Dynamics*, Vol. 26, November-December 2003, pp. 956–971.

[8] D.-W. Gim and K. T. Alfriend, "Satellite Relative Motion using Differential Equinoctial Elements," *Celestial Mechanics and Dynamical Astronomy*, Vol. 92, August 2005, pp. 295–336.

[9] P. Sengupta, S. R. Vadali, and K. T. Alfriend, "Second-order State Transition for Relative Motion near Perturbed, Elliptic Orbits," *Celestial Mechanics and Dynamical Astronomy*, Vol. 97, February 2007, pp. 101–129.

[10] J. A. Kechichian, "The Analysis of the Relative Motion in General Elliptic Orbit with respect to a Dragging and Precessing Coordinate Frame," *Proceedings of the AAS/AIAA Astrodynamics Conference*, Sun Valley, ID, 1997, pp. 2053–2074.

[11] T. A. Lovell and S. G. Tragesser, "Guidance for Relative Motion of Low Earth Orbit Spacecraft based on Relative Orbit Elements," *AIAA/AAS Astrodynamics Specialist Conference*, Providence, Rhode Island, 2004.

[12] S. S. Vaddi, K. T. Alfriend, S. R. Vadali, and P. Sengupta, "Formation Establishment and Reconfiguration Using Impulsive Control," *Journal of Guidance, Control and Dynamics*, Vol. 28, March-April 2005, pp. 262–268.

[13] H. Schaub and K. Alfriend, "J_2 Invariant Relative Orbits for Spacecraft Formations," *Celestial Mechanics and Dynamical Astronomy*, Vol. 79, February 2001.

[14] S. R. Vadali, H. Schaub, and K. T. Alfriend, "Initial Conditions and Fuel-Optimal Control for Formation Flying of Satellites," *AIAA Guidance, Navigation, and Control Conference and Exhibit*, Portland, OR, 1999.

[15] D. Mishne, "Formation Control of Satellites Subject to Drag Variations and J_2 Perturbations," *Journal of Guidance, Control and Dynamics*, Vol. 27, July-August 2004, pp. 685–692.

[16] I. Beigelman and P. Gurfil, "Optimal Fuel-Balanced Impulsive Formationkeeping for Perturbed Spacecraft Orbits," *Journal of Guidance, Control and Dynamics*, Vol. 31, September-October 2008, pp. 1266–1283.

[17] D. A. Vallado, *Fundamentals of Astrodynamics and Applications*. McGraw-Hill Inc., 1997.

[18] K. Alfriend, S. Vadali, P. Gurfil, J. How, and L. Breger, *Spacecraft Formation Flying: Dynamics,Control and Navigation*. Elseiver, Oxford, UK, 2010.

[19] P. Gurfil, *Modern Astrodynamics*. Elseiver, Oxford, UK, 2006.

[20] R. Battin, *An Introduction to the Mathematics and Methods of Astrodynamics*. AIAA Education Series, 1987.